

An Ultra-sensitive Ratiometric Fluorescent Thermometer Based on Monomer and Excimer Dual Emission

Weixu Feng,* Yanhui Wu, Dong Chen, Sumin Lu, Yan Zhao and Hongxia Yan*

Xi'an Key Laboratory of Hybrid Luminescent Materials and Photonic Device, School of Chemistry and Chemical engineering, Northwestern Polytechnical University, Xi'an 710129, Shaanxi, China.

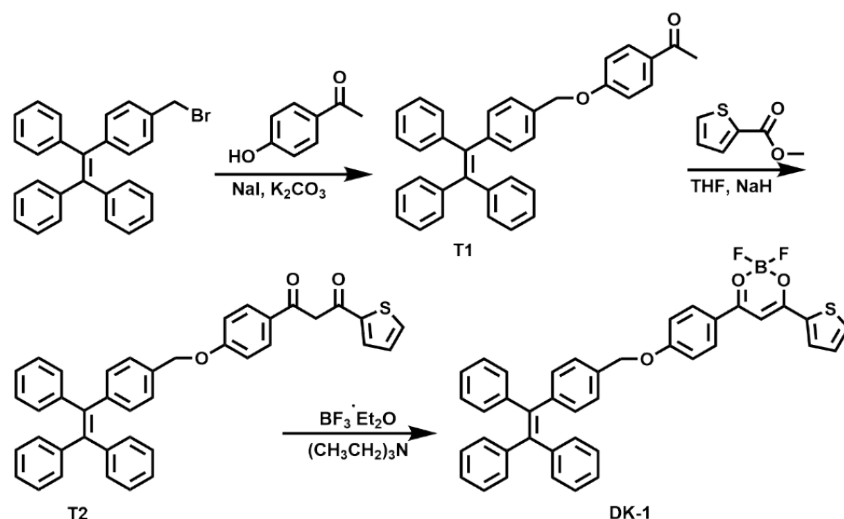
Email: fwxdk@nwpu.edu.cn; hongxiayan@nwpu.edu.cn

Materials and Methods

All manipulations of air and water sensitive compounds were carried out under dry N₂ using the standard Schlenk line techniques. ¹H NMR spectra were recorded on a Bruker Plus 400 spectrometer with SiMe₄ as the internal standard in CDCl₃ and/or DMSO- δ_6 at room temperature. Electronic absorption spectra in the UV/Visible region were recorded with a Shimadzu UV-3159 UV-Vis-NIR spectrophotometer. Emission and excitation spectra in solid state or solution were collected through Hitachi F-7000 spectrometer. The absolute fluorescence quantum yield and lifetime were measured on a combined fluorescence lifetime and steady-state spectrometer (FLS-1000, Edinburgh). Powder X-ray diffraction (PXRD) data were measured by Bruker-D8 Advance. Thermogravimetric analyses (TGA) were performed with a TA thermal analyzer (Q50) under N₂/air with a heating rate of 20 °C/min from 30 to 1000 °C; the sample was

heated under flowing nitrogen/air (40 mL/min). Differential scanning calorimetry (DSC) curves were obtained with a NETZSCH thermal analyzer (DSC 204) at a heating rate of 25 °C/min from 25 to 300 °C under flowing nitrogen. Mass spectrometric studies were performed in the positive ion mode using a quadrupole mass spectrometer (Micromass, Platform II) equipped with a Waters 616HPLC pump. Crystallographic data for DK-1 were obtained using a Bruker-AXS SMART APEX2 CCD diffractometer. MoK α radiation ($\lambda = 0.7107 \text{ \AA}$) was employed for data collection. The structures were initially solved using direct methods and subsequently refined using the full-matrix least-squares method on F² via the SHELXTL package. Refinement of all non-hydrogen atoms incorporated anisotropic thermal parameters, while hydrogen atoms were generated geometrically. Comprehensive crystal data and results of structure refinement can be found in Tables S1. Access to supplementary crystallographic data for CCDC 2290846 is available free of charge through the Cambridge Crystallographic Data Center. The Commission International de l'Eclairage (CIE) coordinates of each sample were calculated on the basis of the international CIE standards. The relative sensitivity (Sr) was calculated via the equation^{S1}: $Sr = 1/\Delta \cdot |\partial\Delta/\partial T|$; The temperature resolution (δT) can be calculated via the equation^{S2}: $\delta T = (1/Sr) \cdot (\partial\Delta/\Delta)$, where the $\partial\Delta/\Delta$ is the relative error of the fluorescence spectrometer. The $\partial\Delta/\Delta$ value (0.033%) was calculated according to the signal to noise ratio of the fluorescence spectrometer (6000:1).^{S3}

Calculation of the molecular electron density distribution by TD-DFT methods. The theoretical calculations were performed using Gaussian 09 program package. The B3LYP approach was chosen as the QM method for geometric optimizations in the S₀ state while the TD-B3LYP approach was applied for geometric optimizations in the S₁ states. In all TDDFT calculations, the 6-31G* basis set was used for all the remaining atoms.



Scheme S1. Synthesis procedures for the **DK-1**.

Synthesis of T1

To a suspension of (2-(4-(bromomethyl)phenyl)ethene-1,1,2-triyl)tribenzene (425.4 mg, 1.0 mmol), 4-hydroxyacetophenone (123.9 mg, 0.91 mmol), NaI (28.5 mg, 0.2 mmol) and K₂CO₃ (186.6 mg, 1.35 mmol) in acetone (10 ml). The mixture was stirred for overnight at room temperature. Pour the reaction solution into the separating funnel, separate the organic phase with ethyl acetate and water, and repeat for three times. Then dry the organic phase with anhydrous Na₂SO₄, and spin the solution until it is dry. Column separation; Petroleum ether: ethyl acetate = 3:1. Yield: 332.4 mg (76%). ¹HNMR (400MHz, CDCl₃, δ, ppm): 2.56 (s, 3H), 5.03 (s, 2H), 7.02-7.11 (m, 21H), 7.92 (d, *J* = 8.8 Hz, 2H). ¹³C NMR (101 MHz, CDCl₃, δ, ppm): 26.12, 69.75, 114.31, 126.25, 126.53, 127.41, 127.46, 127.47, 130.26, 130.32, 131.04, 131.06, 131.07, 131.35, 133.89, 140.14, 141.12, 143.28, 143.33, 143.50, 162.41, 196.54.

Synthesis of T2

To a round bottom flask was added compound S1 (480.6 mg, 1.0 mmol) in 5 mL of dry THF. The solution was purged with N₂ for 10 minutes, then NaH (60%) (240.0 mg, 6.0 mmol)

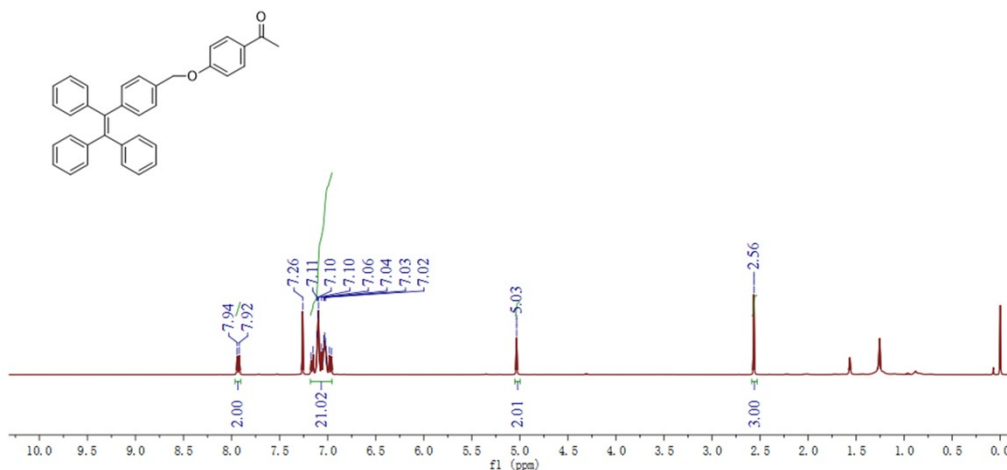


Fig. S1. ¹H NMR spectrum of T1 in CDCl₃ at 298K.

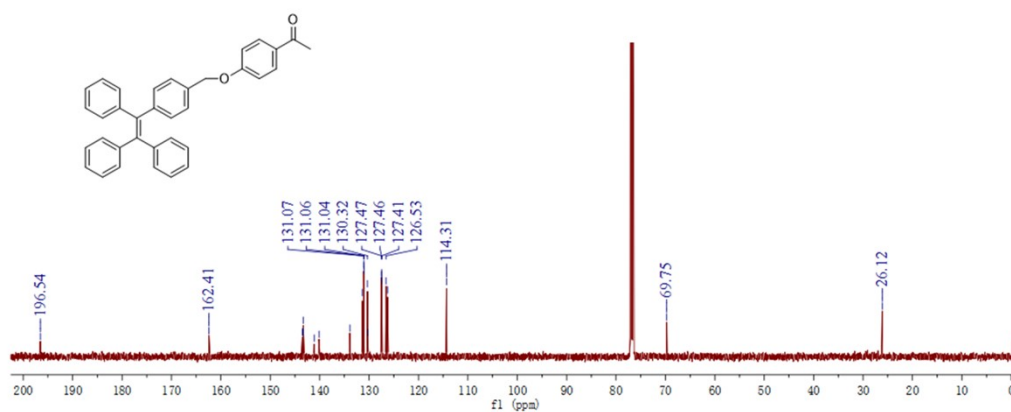


Fig. S2. ¹³C NMR spectrum of T1 in CDCl₃ at 298K.

was added. After stirring for 30 minutes at 65°C under nitrogen, to the mixture was added methyl benzoate (426.5 mg, 3.0 mmol). The reaction mixture was stirred under N₂ protection at 65°C for 24 hours. After cooling to room temperature, the reaction was quenched by careful addition of water in an ice bath. Adjust pH to 7 with HCl (aq). The THF phase was separated and the aqueous suspension was extracted with dichloromethane. The combined organic phases were dried over anhydrous Na₂SO₄, and concentrated under reduced pressure. The crude product was purified by column chromatography (silica gel, 2:1 v/v, petroleum ether/ethyl acetate). Yield: 490.3 mg (83%). ¹H NMR (400MHz, CDCl₃, δ, ppm): 5.05 (s, 2H), 6.63 (s, 1H), 7.02-7.10 (m, 23H), 7.62 (dd, *J*=4.9, 0.7 Hz, 1H), 7.79 (dd, *J*=3.7, 0.8 Hz, 1H), 7.92

(d, $J=8.9$ Hz, 2H). ^{13}C NMR (101 MHz, DMSO-d_6 , δ , ppm): 70.04, 92.14, 114.92, 126.54, 126.86, 127.15, 127.73, 128.29, 128.93, 129.94, 131.34, 131.63, 132.13, 134.19, 140.41, 141.37, 142.20, 143.60, 143.76, 162.28, 181.38, 181.78.

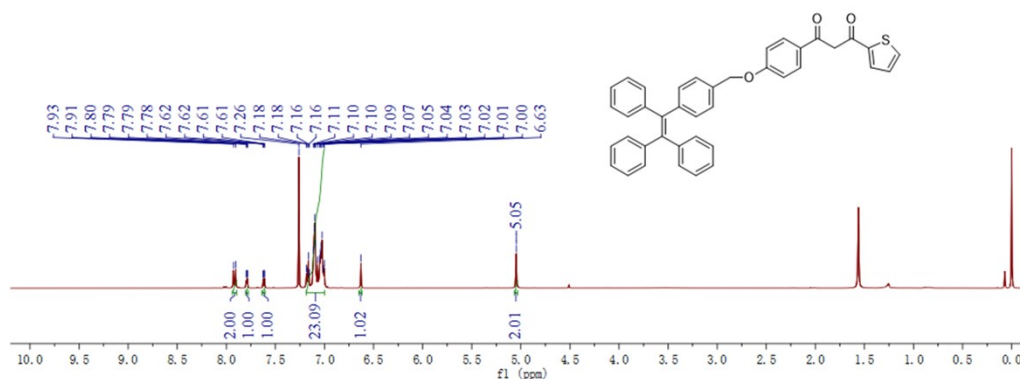


Fig. S3. ^1H NMR spectrum of T2 in CDCl_3 at 298K.

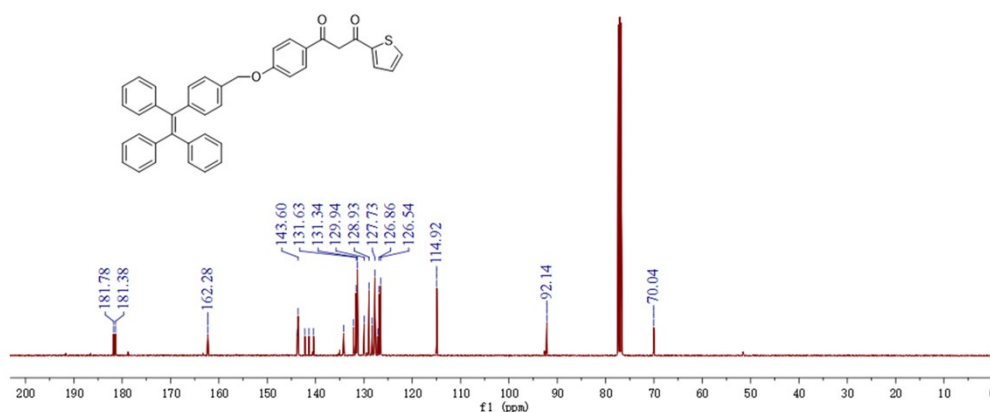


Fig. S4. ^{13}C NMR spectrum of T2 in CDCl_3 at 298K.

Synthesis of DK-1

Triethylamine (0.06 ml, 0.4 mmol) was added to an anhydrous dichloromethane (5 ml) solution of compound S2 (118.1 mg, 0.2 mmol) at room temperature. After stirring for 0.5 hours, $\text{BF}_3 \cdot \text{OEt}_2$ (1.12 ml, 9.0 mmol) was added, and the reaction mixture was stirred for 12 hours without light. The solution was washed with 2M HCl, saturated NaHCO_3 aqueous solution, brine and dried with Na_2SO_4 . After the solvent was removed by rotary evaporation, the residue was purified by column chromatography (silica gel, petroleum ether- CH_2Cl_2 , v/v =

3/2). Yield: 94.5 mg (74%). The crystalline samples for the single crystal measurements were obtained by slow evaporation of a mixed solution of dichloromethane and hexane. $^1\text{H NMR}$ (400MHz, DMSO-d_6 , δ , ppm): 5.19 (s, 2H), 6.98-7.03 (m, 8H), 7.12-7.15 (m, 9H), 7.26 (dd, $J = 8.6, 4.0$ Hz, 4H), 7.46-7.48 (m, 1H), 7.78 (s, 1H), 8.33 (dd, $J = 14.4, 6.9$ Hz, 3H), 8.65 (d, $J = 3.9$ Hz, 1H). $^{13}\text{C NMR}$ (101 MHz, CDCl_3 , δ , ppm): 70.16, 92.12, 115.46, 124.36, 126.55, 126.86, 127.73, 129.30, 131.31, 131.67, 133.57, 134.15, 136.25, 137.36, 140.30, 141.52, 143.48, 144.01, 164.88, 175.27, 181.21. ESI-MS: m/z calculated for $\text{C}_{40}\text{H}_{29}\text{BF}_2\text{O}_3\text{SNa}$ $[\text{M}+\text{Na}]^+$: 661.53, found: 661.59.

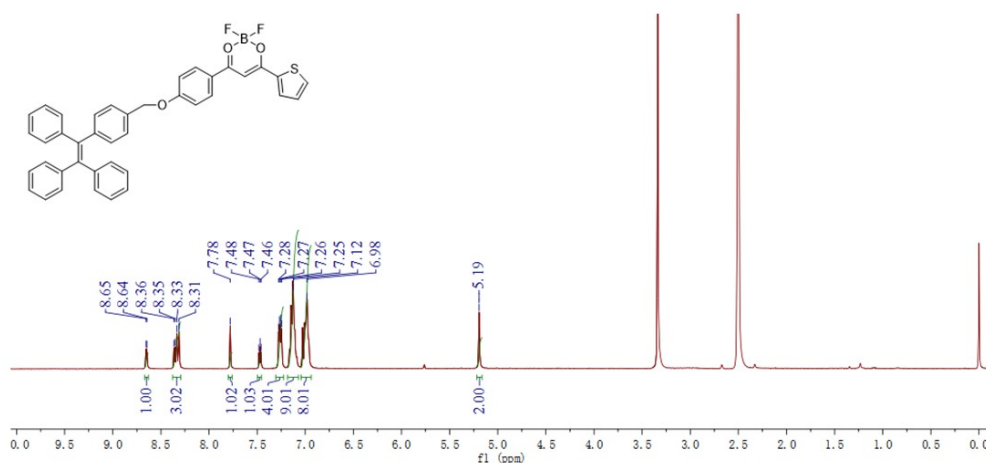


Fig. S5. $^1\text{H NMR}$ spectrum of **DK-1** in DMSO-d_6 at 298K.

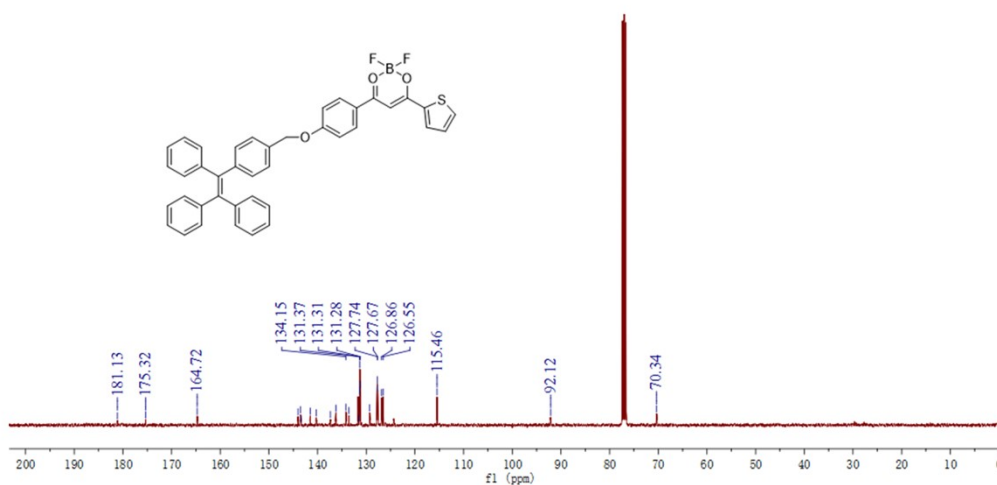


Fig. S6. $^{13}\text{C NMR}$ spectrum of **DK-1** in CDCl_3 at 298K.

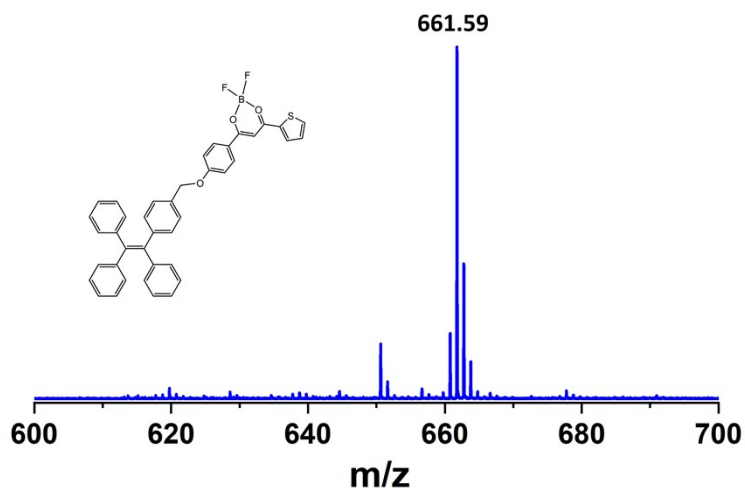
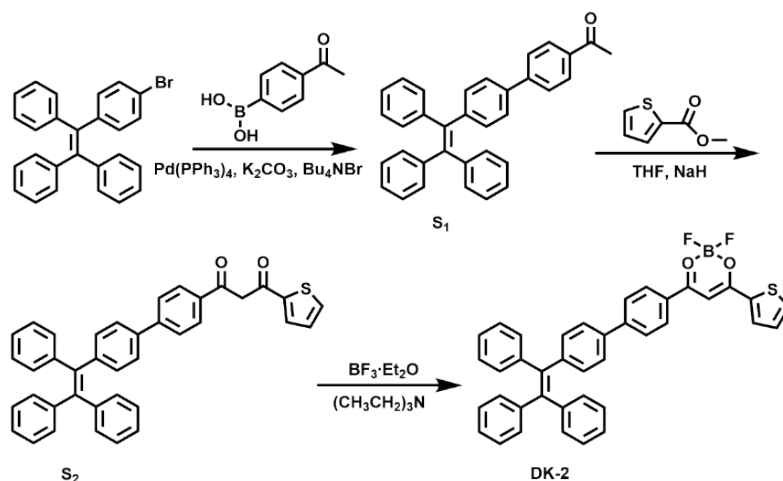


Fig. S7. ESI-MS spectrum of DK-1.



Scheme S2. Synthesis procedures for the DK-2.

Synthesis of S1

Add (2-(4-bromophenyl)ethene-1,1,2-triyl)tribenzene (1.15 g, 2.8 mmol), acetylphenylboronic acid (410.0 mg, 2.5 mmol), Pd[P(C₆H₅)₃]₄ (23.1 mg, 0.02mmol), tetrabutylammonium bromide (451.3 mg, 1.4 mmol), potassium carbonate (690 mg, 5.0 mmol) to the round bottom flask. Add the mixed solution of toluene: H₂O (50ml, v/v = 4/1), heat and reflux at 85 ° under the protection of nitrogen for 24h, cool to room temperature after the reaction, pour the reaction solution into the separating funnel, separate the organic phase with ethyl acetate and water, and repeat for three times. Then dry the organic phase with anhydrous Na₂SO₄, and spin the

solution until it is dry. Column separation; Petroleum ether: ethyl acetate =2:1. Yield: 957.5 mg (85%). $^1\text{H NMR}$ (400MHz, CDCl_3 , δ , ppm): 2.65 (s, 3H), 7.05-7.15 (m, 17H), 7.1 (d, $J=8.3$ Hz, 2H), 7.66 (d, $J=8.3$ Hz, 2H), 8.01 (d, $J=8.3$ Hz, 2H). $^{13}\text{C NMR}$ (101 MHz, CDCl_3 , δ , ppm): 25.61, 125.37, 125.50, 125.55, 125.58, 125.86, 126.63, 126.72, 126.78, 127.82, 130.28, 130.30, 130.35, 130.93, 134.65, 136.41, 139.21, 140.52, 142.52, 142.56, 142.57, 142.88, 144.21, 196.71.

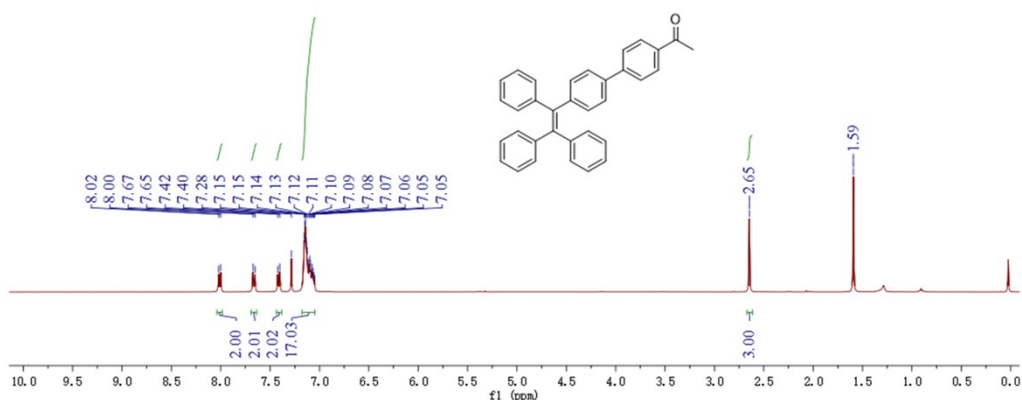


Fig. S8. $^1\text{H NMR}$ spectrum of S1 in CDCl_3 at 298K.

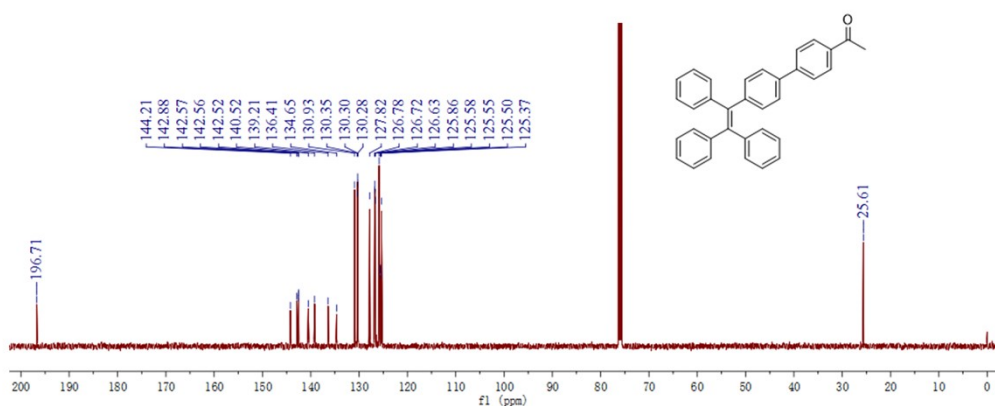


Fig. S9. $^{13}\text{C NMR}$ spectrum of S1 in CDCl_3 at 298K.

Synthesis of S2

To a round bottom flask was added compound S1 (720.9 mg, 1.6 mmol) in 5 mL of dry THF. The solution was purged with N_2 for 10 minutes, then NaH (60%) (336.0 mg, 8.4 mmol) was added. After stirring for 30 minutes at 65°C under nitrogen, to the mixture was added

Fig. S11. ^{13}C NMR spectrum of S2 in CDCl_3 at 298K.

Synthesis of DK-2

Triethylamine (0.06 ml, 0.4 mmol) was added to an anhydrous dichloromethane (5 ml) solution of compound S2 (118.1 mg, 0.2 mmol) at room temperature. After stirring for 0.5 hours, $\text{BF}_3 \cdot \text{OEt}_2$ (1.12 ml, 9.0 mmol) was added, and the reaction mixture was stirred for 12 hours without light. The solution was washed with 2M HCl, saturated NaHCO_3 aqueous solution, brine and dried with Na_2SO_4 . After the solvent was removed by rotary evaporation, the residue was purified by column chromatography (silica gel, petroleum ether- CH_2Cl_2 , v/v = 3/2). Yield: 85.2 mg 70%. ^1H NMR (400MHz, DMSO-d_6 , δ , ppm): 7.08 (ddd, $J=11.8, 8.8, 6.6$ Hz, 6H), 7.17-7.25 (m, 11H), 7.55-7.57 (m, 1H), 7.74 (d, $J=8.3$ Hz, 2H), 7.97-8.02 (m, 3H), 8.42 (d, $J=8.6$ Hz, 2H), 8.48 (d, $J=4.8$ Hz, 1H), 8.80 (d, $J=3.3$ Hz, 1H). ^{13}C NMR (400MHz, CDCl_3 , δ , ppm): 93.33, 126.67, 127.31, 127.82, 129.35, 129.50, 131.36, 132.14, 134.82, 136.73, 137.13, 140.10, 143.52, 144.69, 176.41, 181.18. ESI-MS: m/z calculated for $\text{C}_{39}\text{H}_{28}\text{BF}_2\text{O}_2\text{S}$ $[\text{M}+\text{H}]^+$: 609.52, found: 609.63.

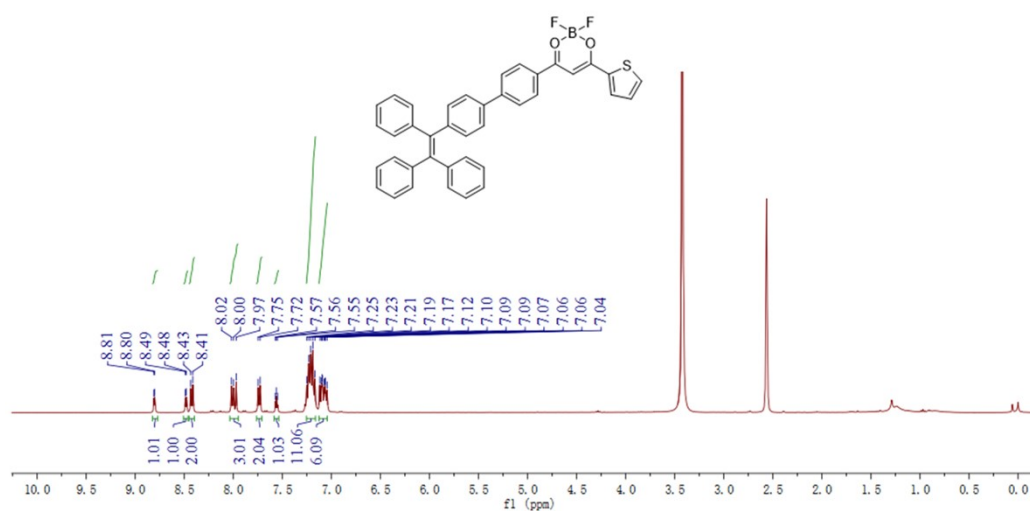


Fig. S12. ^1H NMR spectrum of DK-2 in DMSO-d_6 at 298K.

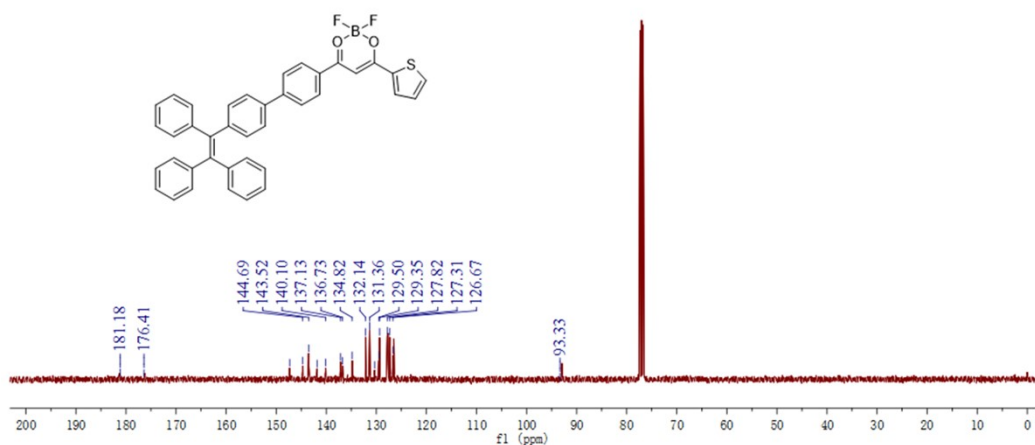


Fig. S13. ^{13}C NMR spectrum of DK-2 in CDCl_3 at 298K.

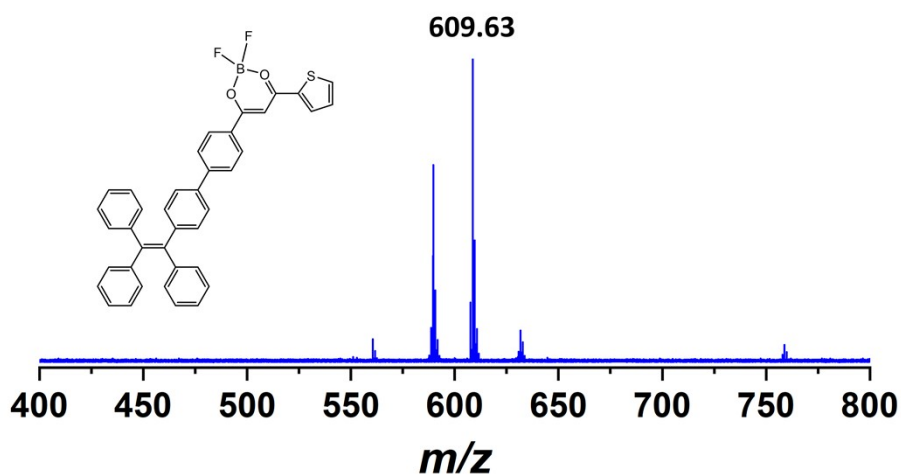


Fig. S14. ESI-MS spectrum of DK-2.

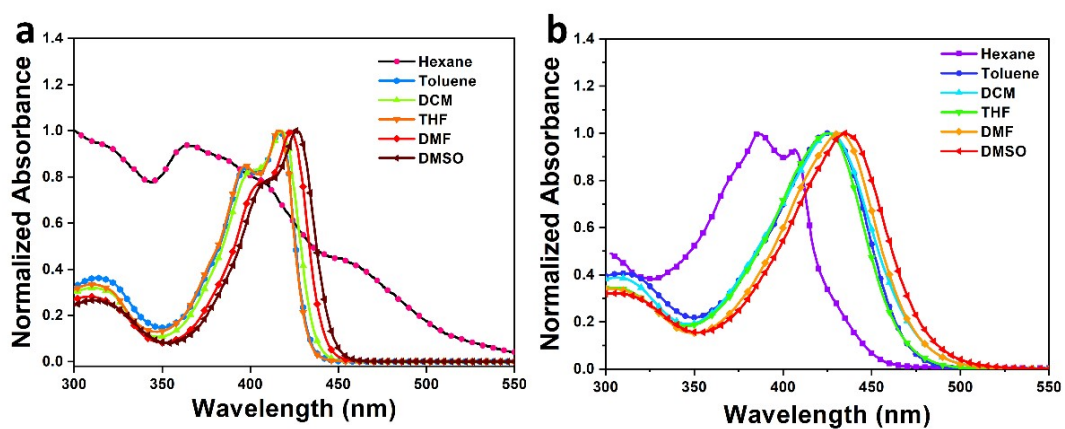


Fig. S15. Uv-vis absorption spectra for (a) DK-1 and (b) DK-2 at different solvents.

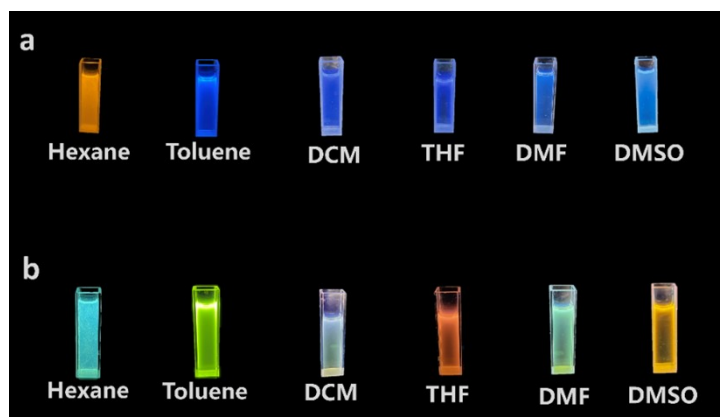


Fig. S16. The digital photographs of (a) DK-1 and (b) DK-2 in solvents of varying polarity under the illumination of a UV lamp ($\lambda_{\text{ex}} = 365 \text{ nm}$).

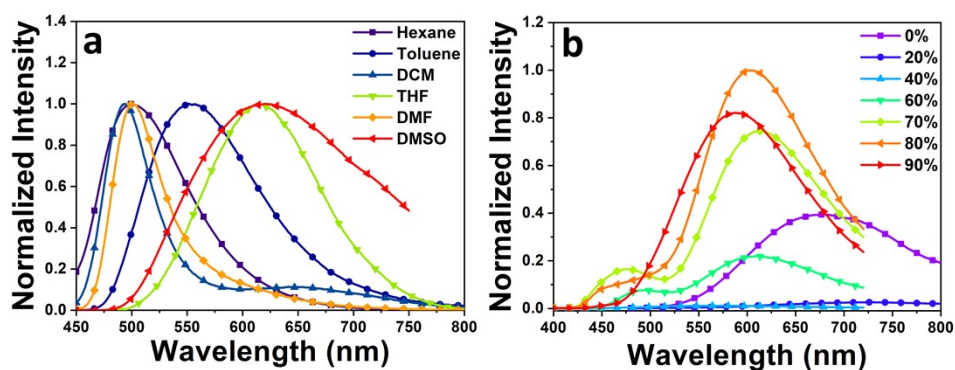


Fig. S17 Normalized emission spectra of (a) DK-2 in various solvents (the concentration is $1 \times 10^{-5} \text{ mol L}^{-1}$); and (b) Fluorescence spectra of DK-2 in THF/water mixtures with different fractions of water. Luminogen concentration: $1 \times 10^{-5} \text{ mol L}^{-1}$.

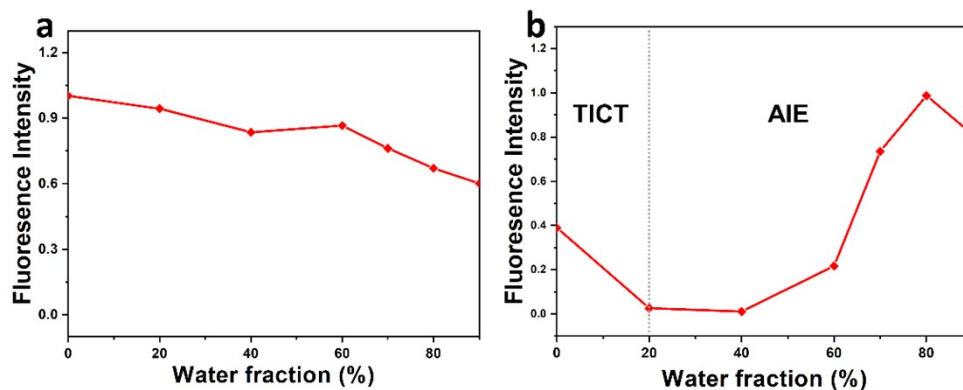


Fig. S18. The dependence of the intensity on the water fraction for the THF solution of (a) DK-1 and (b) DK-2.

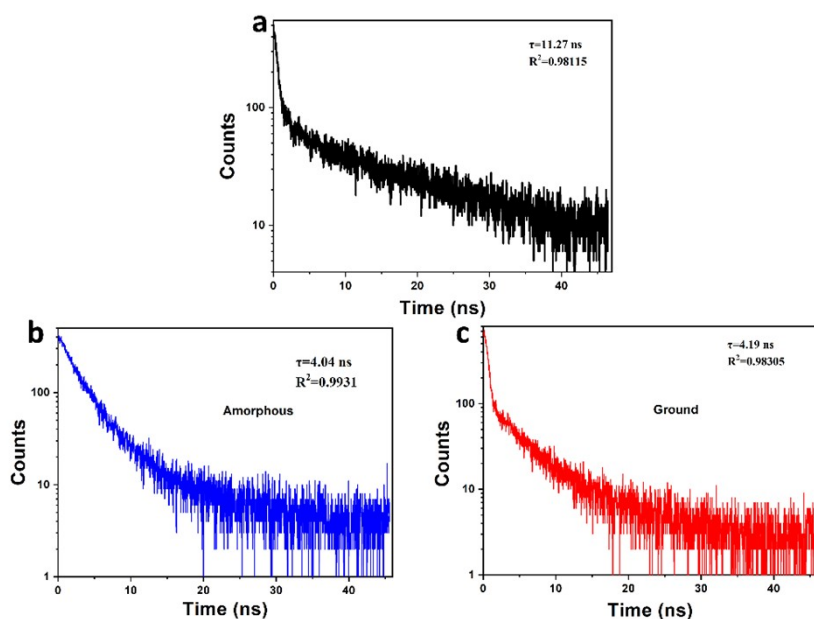


Fig. S19. Luminescence lifetime of (a) **DK-1** at solid state monitored at 619 nm and (b-c) **DK-2** in amorphous state and ground state monitored at 545 nm and 640 nm respectively.

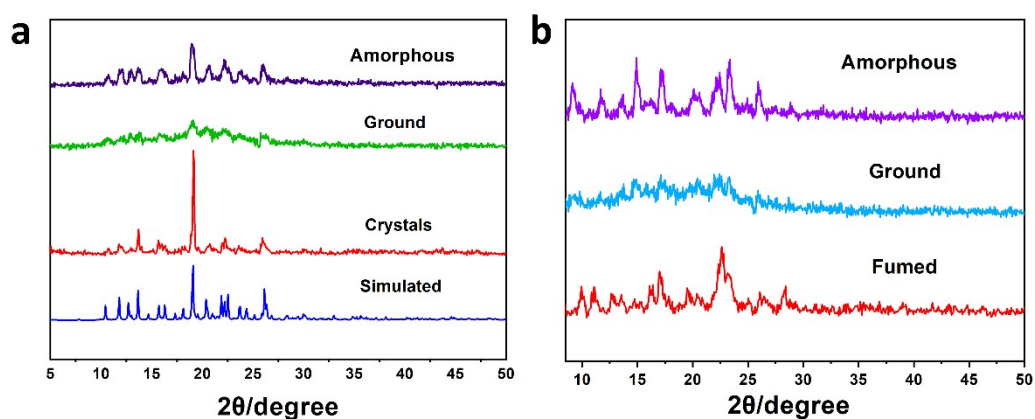


Fig. S20. PXRD patterns of (a) **DK-1** and (b) **DK-2** in different solid states.

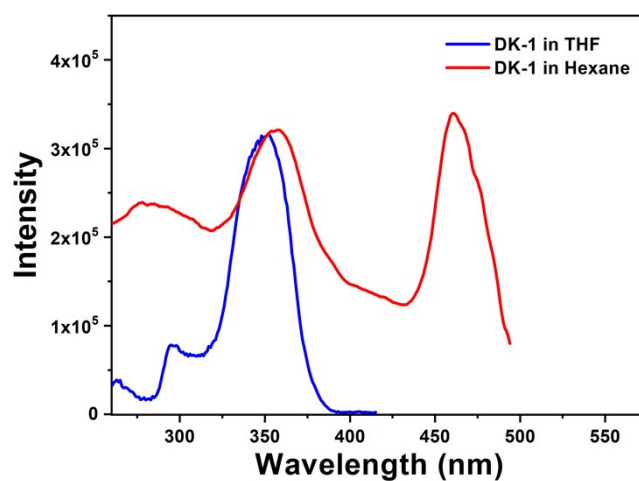


Fig. S21. Excitation spectra for **DK-1** at different solvents.

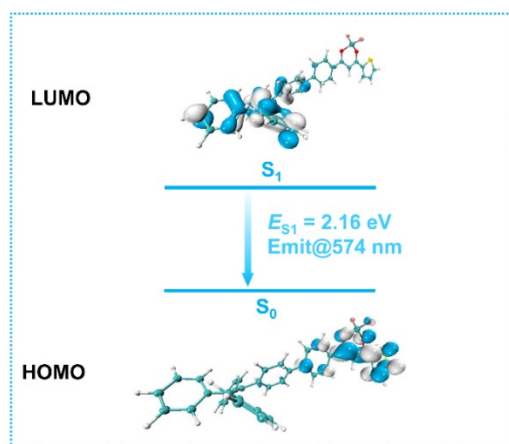


Fig. S22. TD-B3LYP-D3/6-31G* calculated HOMO and LUMO orbital and the corresponding energy (eV) of DK-2.

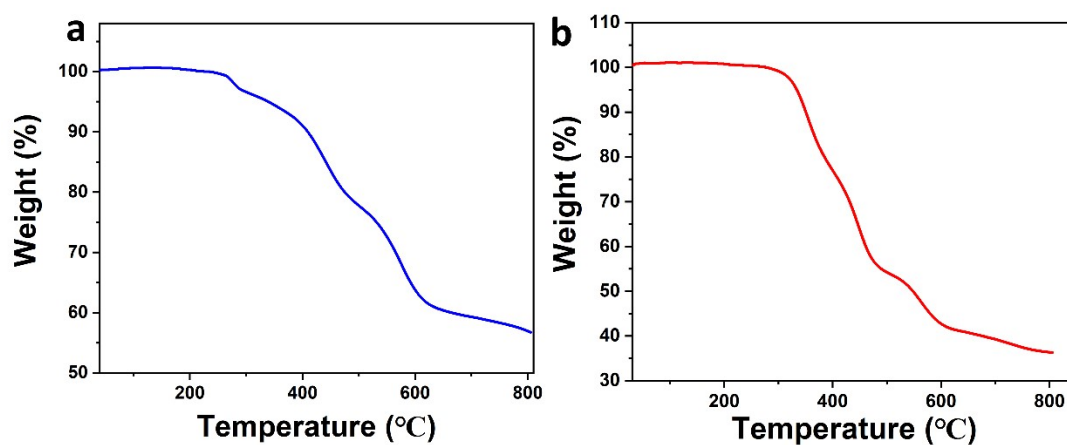


Fig. S23. The TGA curve of (a) DK-1 and (b) DK-2.

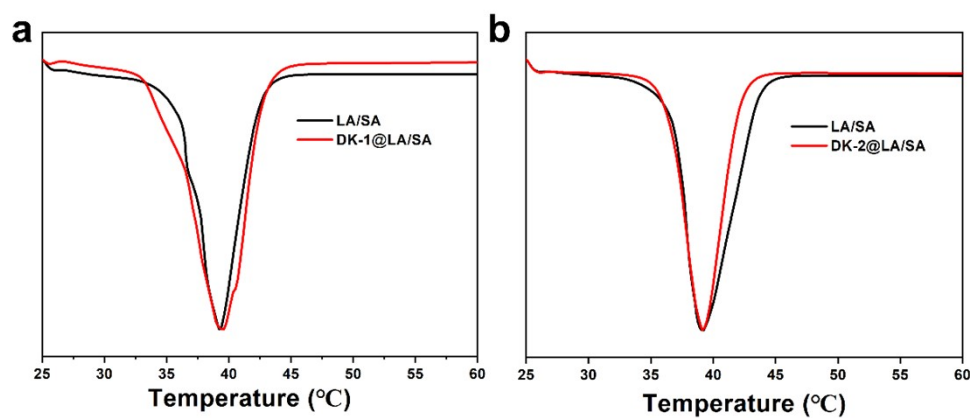


Fig. S24. The DSC curve of (a) pure LA/SA (4:1) and DK-1@LA/SA (0.06%) and (b) pure LA/SA (4:1) and DK-2@LA/SA (0.06%).

Table S1. Crystallographic information on data collection and structure refinement.

Compound	DK-1
Empirical formula	C ₄₀ H ₂₉ BF ₂ O ₃ S
Formula weight	638.50
Crystal system	triclinic
Space group	<i>P</i> -1
<i>a</i> /Å	7.9692(11)
<i>b</i> /Å	9.4628(12)
<i>c</i> /Å	22.723(3)
α /°	84.954(5)
β /°	84.216(6)
γ /°	70.775(5)
<i>V</i> /Å ³	1607.0(4)
<i>Z</i>	2
ρ /g·cm ⁻³	1.320
Temperature (K)	150
Crystal size/mm	0.3*0.1*0.08
μ (Mo-K α)/mm ⁻¹	0.848
Data/restraints/parameters	5654/48/433
Quality-of-fit indicator	1.062
No. unique reflections	5654
	<i>R</i> _{int} =0.0557
	<i>R</i> _{sigma} =0.0510
No. observed reflections	21244
Final <i>R</i> indices [<i>I</i> > 2 σ (<i>I</i>)]	<i>R</i> ₁ =0.0706
	w <i>R</i> ₂ =0.1984
<i>R</i> indices (all data)	<i>R</i> ₁ =0.0951
	w <i>R</i> ₂ =0.2188

Table S2. Fluorescence quantum yield of the DK-1 or DK-2 at solid state.

Sample	PLQY (%)
DK-1 (Amorphous)	8.9
DK-2 (Amorphous)	29
DK-2 (ground)	19.3

Table S3. CIE coordinates of **DK-1@LA/SA** at different temperatures.

Sample	T (°C)	CIE coordinates
DK-1@LA/SA	28	(0.442, 0.382)
	31	(0.429, 0.369)
	34	(0.372, 0.307)
	37	(0.259, 0.188)
	40	(0.252, 0.179)
	43	(0.251, 0.179)
	46	(0.245, 0.177)
	49	(0.245, 0.177)

Table S4. The relative temperature sensing sensitivity of **DK-1@LA/SA** at different temperatures.

Sample	T (°C)	Sr (%)	Resolution (% °C ⁻¹)
DK-1@LA/SA	28	6.19	0.5
	31	12.59	0.3
	34	30.29	0.1
	37	41.25	0.08
	40	2.55	1.3
	43	0.78	4.2
	46	0.75	4.4
	49	0.12	27.5

Table S5. Comparison of the Maximum Relative Sensitivities (Sr) between the present **DK-1@LA/SA** and other thermometers reported recently.

Material	Signal types	Temperature sensing range (°C)	Relative sensitivity (%/°C)	Ref.
Perylene exciplex	Fluorescence ratio	25 – 85	~1	S4
Semiconducting polymer dots	Fluorescence ratio	10 – 70	~1	S5
Quantum dot/quantum rod	Fluorescence ratio	20 – 40	~ 2.4	S6
MOF⊃dye	Fluorescence ratio	20 – 80	maximally up to 1.28	S7
Lanthanide-doped self-assembled polymer monolayers	Fluorescence ratio	23 – 65	maximally up to 1.43	S8
Conjugated polyelectrolytes	Fluorescence ratio	20 -70	0.99 - 2.06	S9
Carbon dot	Lifetime	10 – 45	1.79	S10
Triplet sensitized upconversion	Fluorescence ratio	10 – 50	0.8 - 7.1	S11
FSE	Fluorescence ratio	10 - 70	3.240 - 10.58	S12
Poly-TICT@AIE	Fluorescence Intensity	25-42	17.72	S13
DK-1@LA/SA	Fluorescence ratio	28 - 40	41.25	This work

Table S6. CIE coordinates of DK-2@LA/SA at different temperatures.

Sample	T (°C)	CIE coordinates
DK-2@LA/MA	28	(0.429, 0.502)
	31	(0.428, 0.505)
	34	(0.424, 0.506)
	37	(0.411, 0.506)
	40	(0.365, 0.497)
	43	(0.363, 0.471)
	46	(0.378, 0.481)
	49	(0.388, 0.484)

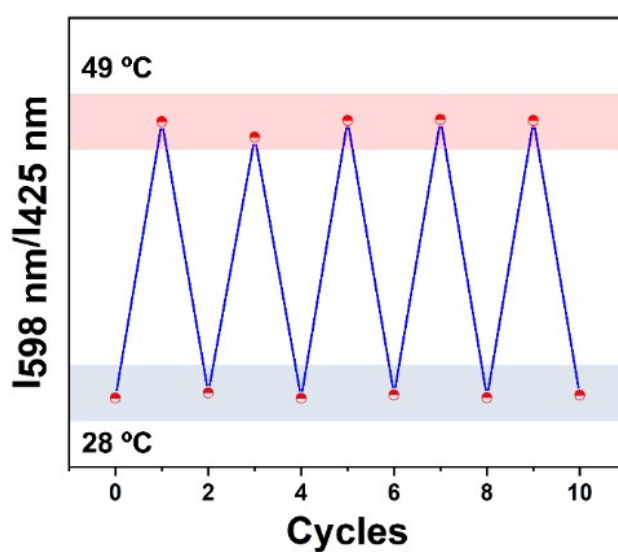


Fig. S25. The “heat-cooling” cycling reversibility of fluorescence with DK-1@LA/SA.

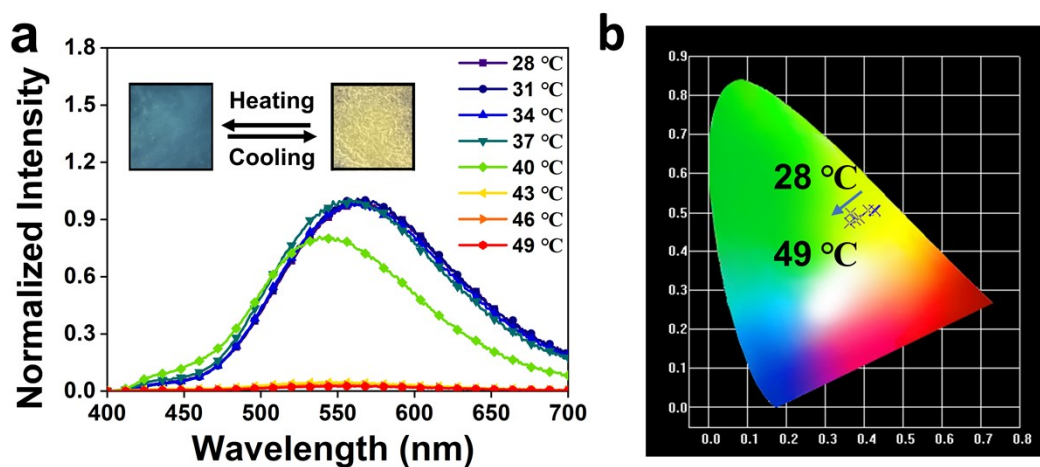


Fig. S26 Emission spectra and CIE coordinates of (a-b) DK-2@LA/SA recorded from 28 °C to 49 °C.

References.

- S1. Cui, Y.; Zhu, F.; Chen, B.; Qian, G. Metal-organic frameworks for luminescence thermometry. *Chem. Commun.* **2015**, *51*, 7420-7431.
- S2. Rocha, J.; Brites, C. D.; Carlos, L. D. Lanthanide Organic Framework Luminescent Thermometers. *Chem. Eur. J.* **2016**, *22*, 14782-14795.
- S3. Zhou, X.; Wang, H.; Jiang, S.; Xiang, G.; Tang, X.; Luo, X.; Li, L.; Zhou, X. Multifunctional Luminescent Material Eu(III) and Tb(III) Complexes with Pyridine-3,5-Dicarboxylic Acid Linker: Crystal Structures, Tunable Emission, Energy Transfer, and Temperature Sensing. *Inorg. Chem.* **2019**, *58*, 3780-3788.
- S4. Chandrasekharan, N.; Kelly, L. A. A dual fluorescence temperature sensor based on perylene/excimer interconversion. *J. Am. Chem. Soc.* **2001**, *123* (40), 9898-9899.
- S5. Ye, F.; Wu, C.; Jin, Y.; Chan, Y.-H.; Zhang, X.; Chiu, D. T. Ratiometric temperature sensing with semiconducting polymer dots. *J. Am. Chem. Soc.* **2011**, *133* (21), 8146-8149.
- S6. Albers, A. E.; Chan, E. M.; McBride, P. M.; Ajo-Franklin, C. M.; Cohen, B. E.; Helms, B. A. Dual-emitting quantum dot/quantum rod-based nanothermometers with enhanced response and sensitivity in live cells. *J. Am. Chem. Soc.* **2012**, *134* (23), 9565-9568.
- S7. Cui, Y.; Song, R.; Yu, J.; Liu, M.; Wang, Z.; Wu, C.; Yang, Y.; Wang, Z.; Chen, B.; Qian, G. Dual-emitting MOF dye composite for ratiometric temperature sensing. *Adv. Mater.* **2015**, *27* (8), 1420-1425.
- S8. Rodrigues, M.; Piñol, R.; Antorrena, G.; Brites, C. D.; Silva, N. J.; Murillo, J. L.; Cases, R.; Díez, I.; Palacio, F.; Torras, N. Implementing Thermometry on Silicon Surfaces Functionalized by Lanthanide-Doped Self-Assembled Polymer Monolayers. *Adv. Funct. Mater.* **2016**, *26* (2), 200-209.
- S9. Darwish, G. H.; Koubeissi, A.; Shoker, T.; Abou Shaheen, S.; Karam, P. Turning the heat on conjugated polyelectrolytes: an off-on ratiometric nanothermometer. *Chem. Commun.* **2016**, *52* (4), 823-826.
- S10. Kalytchuk, S.; Poláková, K. i.; Wang, Y.; Froning, J. P.; Cepe, K.; Rogach, A. L.; Zbořil, R. Carbon dot nanothermometry: intracellular photoluminescence lifetime thermal sensing. *ACS nano* **2017**, *11* (2), 1432-1442.
- S11. Xu, M.; Zou, X.; Su, Q.; Yuan, W.; Cao, C.; Wang, Q.; Zhu, X.; Feng, W.; Li, F. Ratiometric nanothermometer in vivo based on triplet sensitized upconversion. *Nat. commun.*, **2018**, *9* (1), 2698.
- S12. Liang, S.; Wang, Y.; Wu, X.; Chen, M.; Mu, L.; She, G.; Shi, W. An ultrasensitive ratiometric fluorescent thermometer based on frustrated static excimers in the physiological temperature range. *Chem. Commun.* **2019**, *55* (24), 3509-3512.
- S13. Xue, K.; Wang, C.; Wang, J.; Lv, S.; Hao, B.; Zhu, C.; Tang, B. Z. A sensitive and reliable organic fluorescent nanothermometer for noninvasive temperature sensing. *J. Am. Chem. Soc.* **2021**, *143* (35), 14147-14157.